

AN APPLICATION OF FULLY NONLINEAR NUMERICAL WAVE TANK TO THE STUDY ON CHAOTIC ROLL MOTIONS

Katsuji Tanizawa[†] and *Shigeru Naito*[‡]

[†] Ship Research Institute, Tokyo, Japan

[‡] Osaka University, Osaka, Japan

ABSTRACT

A numerical wave tank is applied to the study on chaotic roll motions of two-dimensional floating body. This numerical wave tank is constructed by time domain fully nonlinear simulation method based on potential theory. In this simulation method, boundary value problems both on the velocity potential ϕ and its time derivative $\partial\phi/\partial t$ are solved. The coupling condition between wave and floating body is imposed as the implicit boundary condition of $\partial\phi/\partial t$ on wetted body surface. The radiation condition at the tank ends are satisfied by artificial damping technique.

In the study on chaotic roll motions, simple nonlinear model equations are popularly used and hydrodynamics are taken into consideration as hydrodynamic coefficients. They are usually obtained by linear or weak non-linear theories. But in the study on highly nonlinear hydrodynamic phenomena, there is no proof to validate the applicability of such a classical method even for the qualitative argument. When roll motions are chaotic in regular wave, we are not convinced to use hydrodynamic coefficients corresponding to the incident wave frequency.

The aim of this study is introducing a new technology to the field of nonlinear hydrodynamics and floating body dynamics. Using the numerical wave tank, motions of fluid and floating body can be simulated in time domain taking fully nonlinear fluid-body interaction into account. Simulated time history, phase plot and Poincaré mapping of chaotic roll motions are presented and the dependency of the chaotic motion to wave height, wave length, GM of floating body etc. will be discussed.

KEY WORDS : Chaotic roll motion, Parametric oscillation, Numerical wave tank, Fluid-body interaction, Fully nonlinear simulation, Acceleration potential, Implicit body surface boundary condition

INTRODUCTION

Responses of floating bodies such as ships or ocean structures to incident waves are one of the main concern in ocean engineering. The responses are usually treated as harmonic assuming small amplitude wave and body motions. Under the assumption, the frequency responses have been

investigated by linear or perturbation theories. But, the body motions are not always harmonic in real ocean. When amplitude of wave and body motions are large in rough seas, nonlinear effects become dominant. Capsizing in the plunging breaker is the extreme example. Even if the amplitudes are small, nonlinearity due to body shape, mooring force, free water on the deck etc. affect to the body motions and parametric or chaotic motions may be resulted.

For the analysis of such a nonlinear roll motions, time domain fully nonlinear simulation can be a powerful tool. Time domain fully nonlinear simulation methods are studied by Vinje ³⁾, Cointe ⁵⁾, Tanizawa ^{6, 12, 13)}, Van Daalen ⁸⁾, Sen ⁹⁾, Cao ¹⁰⁾, Francescutto ⁷⁾ and others in the past decade and fully nonlinear numerical wave tanks have been developed.

In our previous study ⁷⁾, we applied the numerical wave tank to the analysis of parametric roll motions of bow section body and showed the simulated harmonic and parametric motions, critical wave height of the parametric excitation, etc. are well agree with the experimental results. In this study, we apply the same numerical wave tank to the analysis of chaotic roll motions and the applicability is examined.

FULLY NONLINEAR NUMERICAL WAVE TANK

Mathematical formulation

Motions of a floating body inside a two-dimensional wave basin is considered. As Fig.1 shows, fluid domain is bounded by free-surfaces S_{f1} , a piston wave maker S_p , bottom and rigid wall S_b and a floating body S_s . Here, gravitational acceleration g , density of outside fluid ρ and width of floating body B are chosen as units to nondimensionalize the problem. An space-fixed Cartesian coordinate system $o-xz$ is used with x coincident with the calm free-surface and z positive upward. The fluid is assumed to be homogeneous, incompressible, inviscid and its motion irrotational. The fluid motion can be described by a velocity potential ϕ and its time derivative ϕ_t . In the fluid domain, ϕ and ϕ_t satisfies Laplace's equation

$$\nabla^2\phi = \nabla^2\phi_t = 0 . \quad (1)$$

Green's second identity can be applied on both ϕ and ϕ_t

$$c(\mathcal{Q}) \left\{ \begin{array}{l} \phi(\mathcal{Q}) \\ \phi_t(\mathcal{Q}) \end{array} \right\} = \int_S \left\{ \begin{array}{l} \phi(\mathcal{P}) \\ \phi_t(\mathcal{P}) \end{array} \right\} \frac{\partial}{\partial n} \ln r(\mathcal{P}, \mathcal{Q}) \\ - \ln r(\mathcal{P}, \mathcal{Q}) \left\{ \begin{array}{l} \frac{\partial\phi(\mathcal{P})}{\partial n} \\ \frac{\partial\phi_t(\mathcal{P})}{\partial n} \end{array} \right\} dS , \quad (2)$$

where \mathcal{P}, \mathcal{Q} are points on the boundary, n is outward normal direction of the boundary, $r(\mathcal{P}, \mathcal{Q})$ is distance between \mathcal{P} and \mathcal{Q} , $c(\mathcal{Q})$ represents the angle subtended at \mathcal{Q} by boundaries.

On the free-surface, kinematic boundary condition and dynamic boundary condition for zero atmospheric pressure are applied as

$$\frac{D\phi}{Dt} = -z + \frac{1}{2}(\nabla\phi)^2 \quad (3)$$

$$\frac{D\mathbf{x}}{Dt} = \nabla\phi , \quad (4)$$

where $\mathbf{x} = (x, z)$. On the body surface, impermeability condition with respect to ϕ is expressed as

$$\frac{\partial\phi}{\partial n} = V_n , \quad (5)$$

where V_n denotes the normal velocity of the body surface S_s . Denoting translating and angular velocities of the body as \mathbf{v}_0 and $\boldsymbol{\omega}$ respectively, V_n is written as

$$V_n = \mathbf{n} \cdot (\mathbf{v}_0 + \boldsymbol{\omega} \times \mathbf{r}) . \quad (6)$$

Impermeability condition on the body with respect to ϕ_t ¹²⁾ can be written as

$$\begin{aligned} \frac{\partial \phi_t}{\partial n} = & -k_n (\nabla \phi - \mathbf{v}_0 - \boldsymbol{\omega} \times \mathbf{r})^2 + \mathbf{n} \cdot (\dot{\mathbf{v}}_0 + \dot{\boldsymbol{\omega}} \times \mathbf{r}) \\ & + \mathbf{n} \cdot \boldsymbol{\omega} \times (\boldsymbol{\omega} \times \mathbf{r}) + \mathbf{n} \cdot 2\boldsymbol{\omega} \times (\nabla \phi - \mathbf{v}_0 - \boldsymbol{\omega} \times \mathbf{r}) \\ & - \frac{\partial}{\partial n} \left(\frac{1}{2} (\nabla \phi)^2 \right) , \end{aligned} \quad (7)$$

where k_n is curvature of body, $\dot{\mathbf{v}}_0, \dot{\boldsymbol{\omega}}$ are translating and angular accelerations of the body respectively.

On the floating body surface, $\dot{\mathbf{v}}_0, \dot{\boldsymbol{\omega}}$ can not be specified explicitly and implicit boundary condition should be applied ¹²⁾. Denoting the inertia tensor of the floating body as \mathcal{M} and generalized normal vector of body surface as $\mathbf{N} = (\mathbf{n}, \mathbf{n} \times \mathbf{r})$, the implicit boundary condition is written as

$$\begin{aligned} \frac{\partial \phi_t}{\partial n} = & \mathbf{N} \mathcal{M}^{-1} \int_{S_s} -\phi_t \mathbf{N} ds \\ & + \mathbf{N} \mathcal{M}^{-1} \left\{ \int_{S_s} \left(-z - \frac{1}{2} (\nabla \phi)^2 \right) \mathbf{N} ds + \mathbf{F}_g \right\} \\ & + q - \frac{\partial}{\partial n} \left(\frac{1}{2} (\nabla \phi)^2 \right) , \end{aligned} \quad (8)$$

where \mathbf{F}_g is sum of gravity, mooring force and other external forces acts to the body and q is the term which can be explicitly evaluated from the solution of velocity field as

$$\begin{aligned} q = & -k_n (\nabla \phi - \mathbf{v}_0 - \boldsymbol{\omega} \times \mathbf{r})^2 \\ & + \mathbf{n} \cdot \boldsymbol{\omega} \times (\boldsymbol{\omega} \times \mathbf{r}) + \mathbf{n} \cdot 2\boldsymbol{\omega} \times (\nabla \phi - \mathbf{v}_0 - \boldsymbol{\omega} \times \mathbf{r}) . \end{aligned} \quad (9)$$

With these boundary conditions and Green's second identity with respect to ϕ and ϕ_t , both velocity and acceleration fields can be solved numerically by BEM. The solutions are integrated with respect to time by 4th order Runge-Kutta method, then fluid and the body motions are simulated in time domain. The free-surface is traced by MEL ²⁾.

Artificial damping zone

Following a preceding work of Cointe et al. ⁵⁾, damping terms are added to dynamic and kinematic free-surface boundary conditions to give artificial damping effect to free-surface. The free-surface boundary conditions inside a damping zone are given as

$$\frac{D\phi}{Dt} = -z + \frac{1}{2} (\nabla \phi)^2 - \nu(x_\epsilon) (\phi - \phi_\epsilon) \quad (10)$$

$$\frac{D\mathbf{x}}{dt} = \nabla \phi - \nu(x_\epsilon) (\mathbf{x} - \mathbf{x}_\epsilon) . \quad (11)$$

where $\nu(x_\epsilon)$ is the damping coefficient

$$\nu(x) = \begin{cases} \alpha \omega \left(\frac{x - x_0}{\lambda} \right)^2, & \text{for } x_0 \leq x \leq x_1 = x_0 + \beta \lambda \\ 0, & \text{for } x < x_0 \text{ or } x > x_1 \end{cases} . \quad (12)$$

In the definition of $\nu(x)$, ω and λ are angular frequency and wave length of the incident wave respectively. The performance of this damping zone is controlled by two nondimensional parameter

α and β . α is used to control the strength of damping and β is used to control the length of damping zone. ϕ_e, \mathbf{x}_e are reference values. This damping zone damps down differences $\phi - \phi_e$ and $\mathbf{x} - \mathbf{x}_e$. When the damping zone is applied in front of a rigid wall and works as a simple absorber, the reference values are set to $\phi_e = 0, \mathbf{x}_e = (x_e, 0)$. And when the damping zone is applied in front of a wave maker and works as an absorbing wave maker, the reference values are set to the solution of the wave generated by the wave maker. This solution can be computed by numerical simulation of the wave without bodies in the tank. For practical purpose, linear analytical solution can be a good substitution. Linear propagating wave generated by a piston wave maker is described as

$$\phi(x, z, t) = \frac{4s \tanh kh \sinh kh}{\omega(2kh + \sinh 2kh)} \cosh k(z + h) \cos(kx - \omega t) \quad (13)$$

$$\eta(x, t) = -\left. \frac{\partial \phi}{\partial t} \right|_{z=0} = \frac{4s \sinh^2 kh}{2kh + \sinh 2kh} \sin(kx - \omega t) \quad (14)$$

where s is stroke of the wave maker and k is wave number of the generated wave. Wave reflection coefficient of this damping zone is less than 2%, when the tuning parameter is appropriately set to $\alpha = \beta = 1$ for a regular wave.^{5, 13)}

SIMULATION OF CHAOTIC ROLL MOTIONS

Floating body

Motions of a two dimensional round rectangular body in regular waves are considered. Fig.2 shows the shape of the body. This is a typical shape of midship section of ships. Table.?? shows its principal dimensions. This floating body has very small negative meta-center height and stable heel angle is nearly equal 4 degree in calm water. This means that free rolling of the body has two point attractors. The hydro-static property is shown in Fig.3(a). GZ curve of the body is approximated by following cubic polynomial. The restoring moment of roll motion has strong nonlinearity.

$$GZ \approx -1.69 \times 10^{-3} \theta + 3.53 \times 10^{-1} \theta^3, \quad GZ(m), \theta(\text{radian}) \quad (15)$$

Fig.3(b) is the magnified view of Fig.3(a) and Fig.3(c) is the potential energy.

Simulated body motions

In Fig.??, simulated motions are plotted. Two different body motions can be observed in this figure. In the first stage, harmonic motions are dominant. As time passed, in the second stage, the amplitude of parametric motion is getting larger gradually. Finally, in the third stage, the parametric motions become dominant and are converging to the limit cycle. In this simulation, these three stages are simulated seamlessly. In the parametric stage, the amplitude of sway and roll are much larger than that of in the harmonic stage and double period motions can be observed clearly. To the contrary, the amplitude of heave in parametric stage is smaller than that of harmonic stage. The energy of heave motion is considered to be transferred to the sway motion and mainly to roll motion.

Other two interesting phenomena are observed in the simulated motions. One is the difference of wave drift force between harmonic and parametric stages. In the plot of sway motion, the mean drift distance in parametric stage looks a little larger than that of in harmonic stage. Another is the difference of mean heave level between harmonic and parametric stages. In the harmonic stage, the mean level is identical to zero. But in parametric stage, the mean level is nearly 20% of wave amplitude. This suggests the existence of lifting force in parametric stage. The mechanism of these phenomena is considered to be highly nonlinear and still not clearly understood.

Fig.?? shows the phase plot of simulated motions. Limit cycle of harmonic and parametric stages are clearly observed and the transition stage between them also can be seen clearly. The aspect ratio of these phase plots are set so that the harmonic motions are plotted as a circle. Phase

plot of sway motion looks chaotic but this is due to the slow drift motion and not due to chaotic motion.

To visualize the motion of water, simulated instantaneous profiles of the free-surface inside and outside of the body at $t/T_w = 84.75, 85.50, \dots, 86.50$ are plotted in Fig.8, where T_w is the period of the incident wave. The wave motion outside of the body is not large, but the wave motion inside is quite large. The inside wave generated by internal wall of the body travels from one side and the wash up to the other side. In this simulation, this internal wave motion is also periodically stable and not chaotic.

To have a limit cycle in parametric oscillation, damping force proportional to $\dot{\theta}^2$ or higher is indispensable. But, in general, damping due to wave radiation is so weak that the parametric roll motions are diverging. In the above simulation, the internal wave motion interacts to the body and external wave motion and, as a results, acts as higher order damping to have the limit cycle. This is another interesting result for future study.

CONCLUSION

In this study, applicability of the fully nonlinear numerical wave tank to parametric and chaotic roll motions with internal free water is examined. This topic is still under investigation and following items are tentative conclusion.

1. In a small amplitude regular wave, a harmonic and parametric motion of triangular body with internal water can be simulated seamlessly.
2. In the parametric motions, shift of mean drift force and center of heave motion from the harmonic motions are simulated. The mechanism of these shifts are considered to be highly nonlinear.
3. The limit cycle of parametric motions are obtained. The motion of internal water acts important roll to have this limit cycle.
4. The simulated parametric motions are periodically stable and no sign of chaotic motions are obtained.

We are now trying to catch chaotic roll motions using the numerical wave tank, but have not succeeded yet. Some good indexes to find the condition of chaotic motions are required to avoid trial and error with various wave length, wave height, amount of internal water, Meta-center height and etc.

REFERENCES

- 1) Murashige,S. and Aihara,K. (1997), "Chaotic Motion of a Flooded Ship in Waves", *Tech. Rep. of Math. Eng. Sec. of the Univ. of Tokyo, METR97-01*, pp1-17
- 2) Longuet-Higgins,M.S. and Cokelet,E. (1976), "The deformation of steep surface waves on water", *Proc. Roy. Soc. ser.A350*, pp1-26
- 3) Vinje, T. and Brevig, P. (1981), "Nonlinear Ship Motions", *Proc. of the 3rd. Int. Conf. on Num. Ship Hydro.*, ppIV3-1-IV3-10
- 4) Sen, D., Pawlowski, J.S., Lever, J. and Hinchey, M.J., (1989), "Two-dimensional numerical modeling of large motions of floating bodies in waves", *Proc. 5th Int. Conf. Num. Ship Hydro., part1*, pp257-277
- 5) Cointe,R.,Geyer,P.,King,B.,Molin,B. and Tramoni,M. (1990), "Nonlinear and linear motions of a rectangular barge in perfect fluid", *Proc. of the 18th Symp. on Naval Hydro., AnnArbor, Michigan*, pp85-98
- 6) Tanizawa, K. (1990), "A numerical method for nonlinear simulation of 2-D body motions in waves by means of B.E.M.", *Journal of SNAJ*, Vol.168, pp223-228
- 7) Kang,C.G., and Gong,I.Y. (1990), "A numerical solution method for three-dimensional nonlinear free-surface problems", *Proc. of the 18th Symp. on Naval Hydro., Annbor, Michigan.*, pp427-438

- 8) Van Daalen, E.F.G. (1993), "Numerical and Theoretical Studies of Water Waves and Floating Bodies", *Ph.D. thesis, University of Twente, The Netherlands*
- 9) Sen, D. (1993), "Numerical simulation of motions of two-dimensional floating bodies", *Journal of Ship Research, vol.37*, pp307-330
- 10) Cao, Y., Beck, R. and Schultz, W.W. (1994), "Nonlinear motions of floating bodies in incident waves", *9th Workshop on Water Waves and Floating Bodies, Kuju, Oita*, pp33-37
- 11) Tanizawa, K. (1995a) "A Nonlinear Simulation Method of 3-D body Motions in Waves", *10th Workshop on Water Waves and Floating Bodies, Oxford*, pp235-239
- 12) Tanizawa, K. (1995b) "A Nonlinear Simulation Method of 3-D Body Motions in Waves", *Journal of SNAJ, Vol.178*, pp179-191
- 13) Tanizawa, K. (1996) "Long time fully nonlinear simulation of floating body motions with artificial damping zone", *Journal of SNAJ, Vol.180*, pp311-319

Table 1: Principal dimensions

Floating Body		
Breadth	B	0.740 m
Draft	d	0.415 m
Weight	W	184.3 kg
Radius of inertia	R_I	0.266 m
Meta-center height	GM	-0.00043 m
Spring constant of mooring	k	51.07 N
Damping coef. of mooring	c	21.40 N/(m/s)

Fig.1: Numerical Wave Tank

Fig.2: Shape of Floating Body

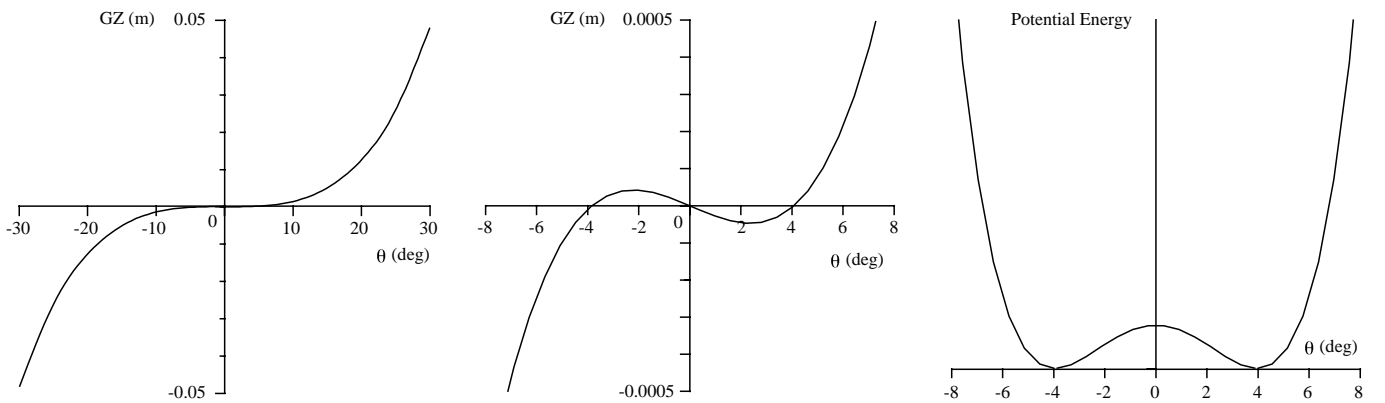


Fig.3: GZ Curve of the Floating Body

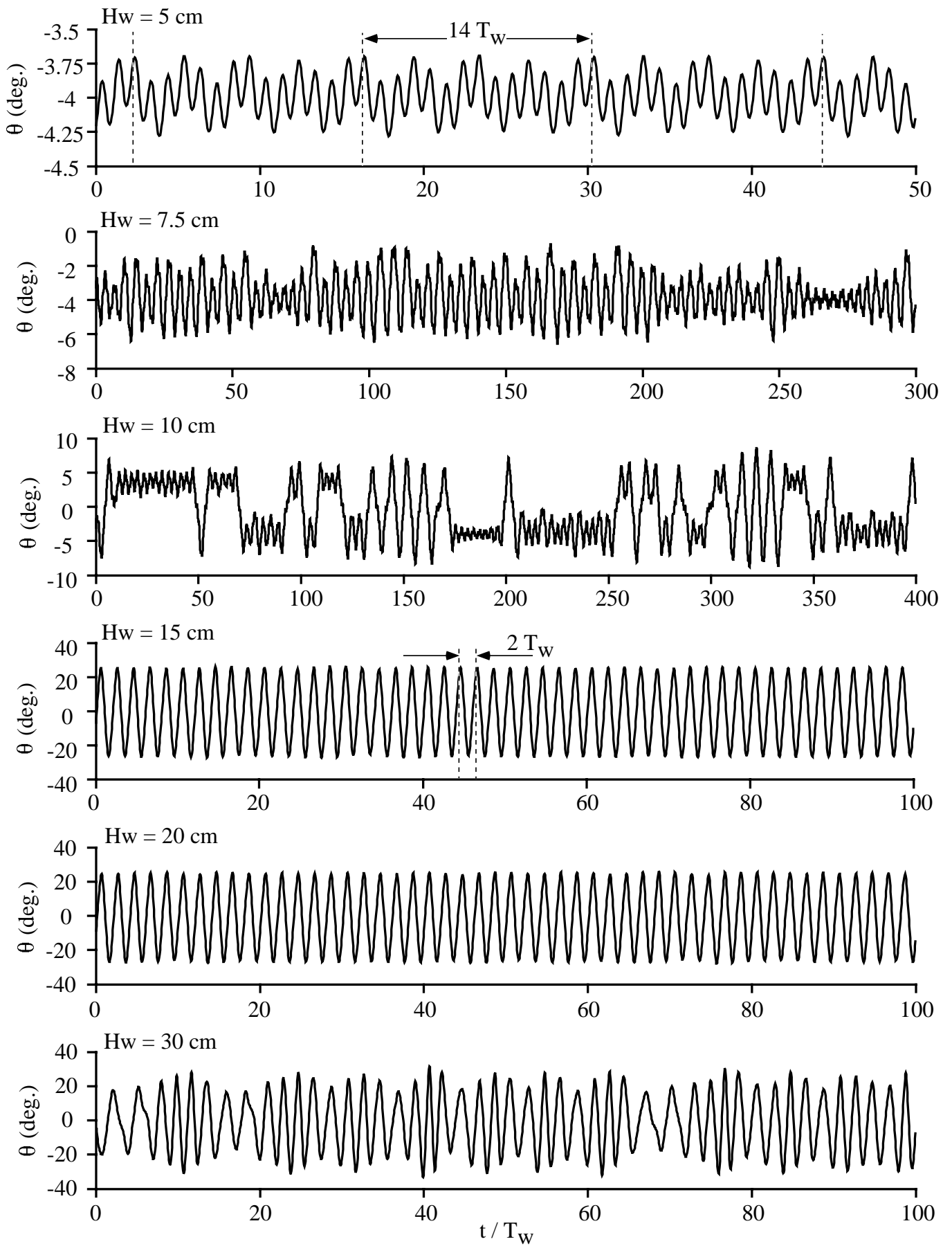


Fig.4: Simulated time histories of the roll motion

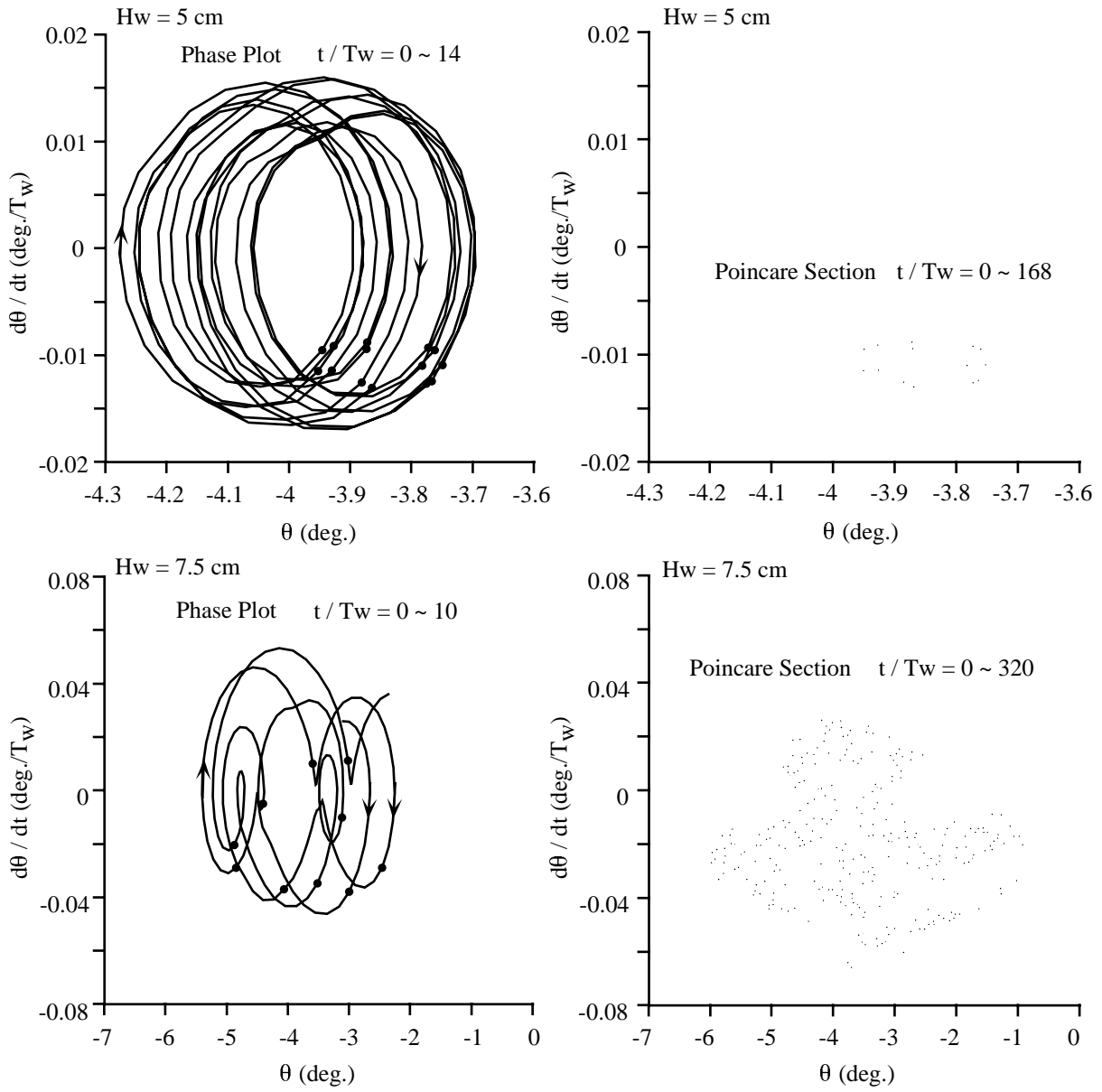


Fig.5: Phase plot and its Poncare section of the simulated roll motion

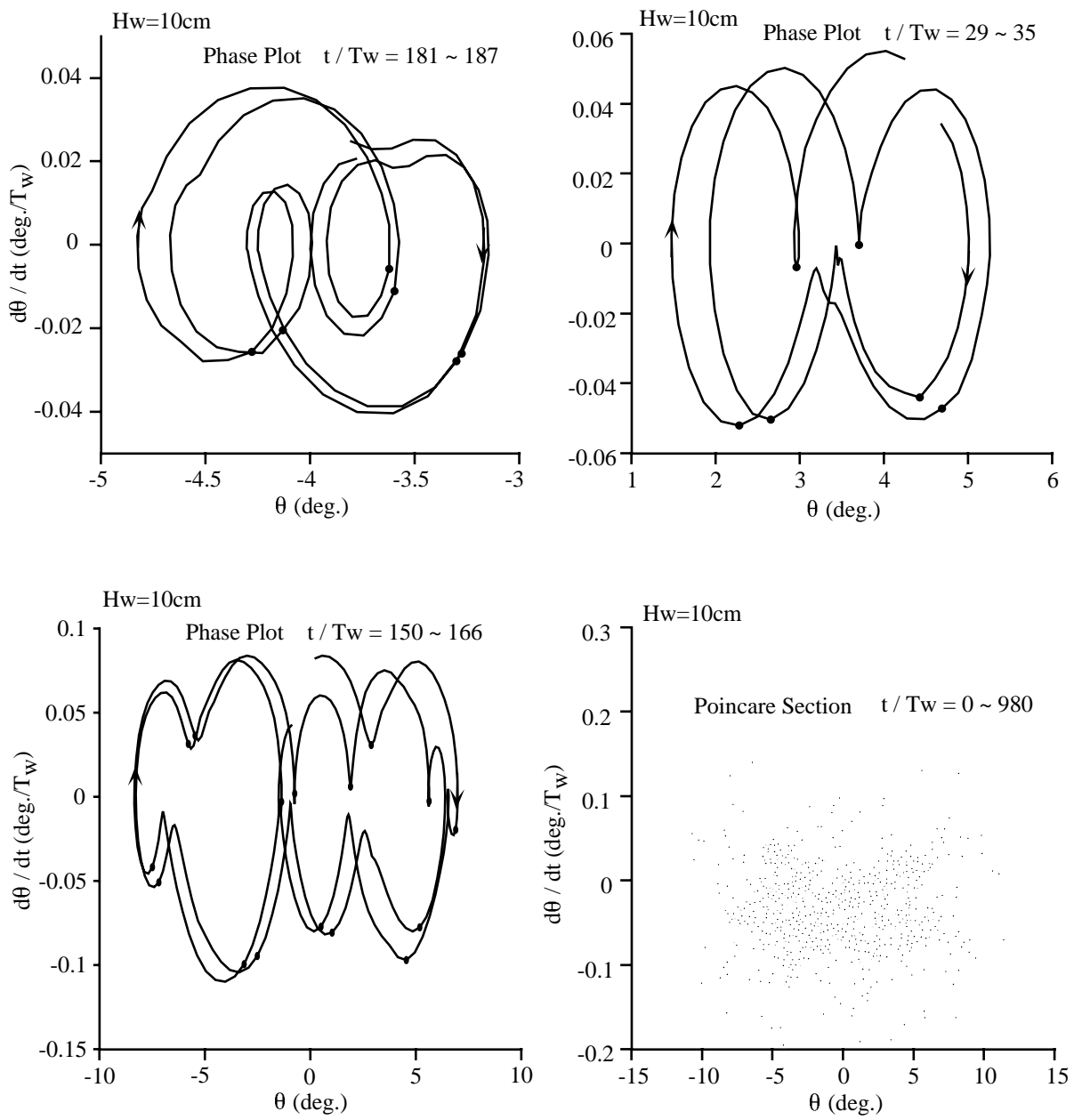


Fig.6: Phase plot and its Poncare section of the simulated roll motion

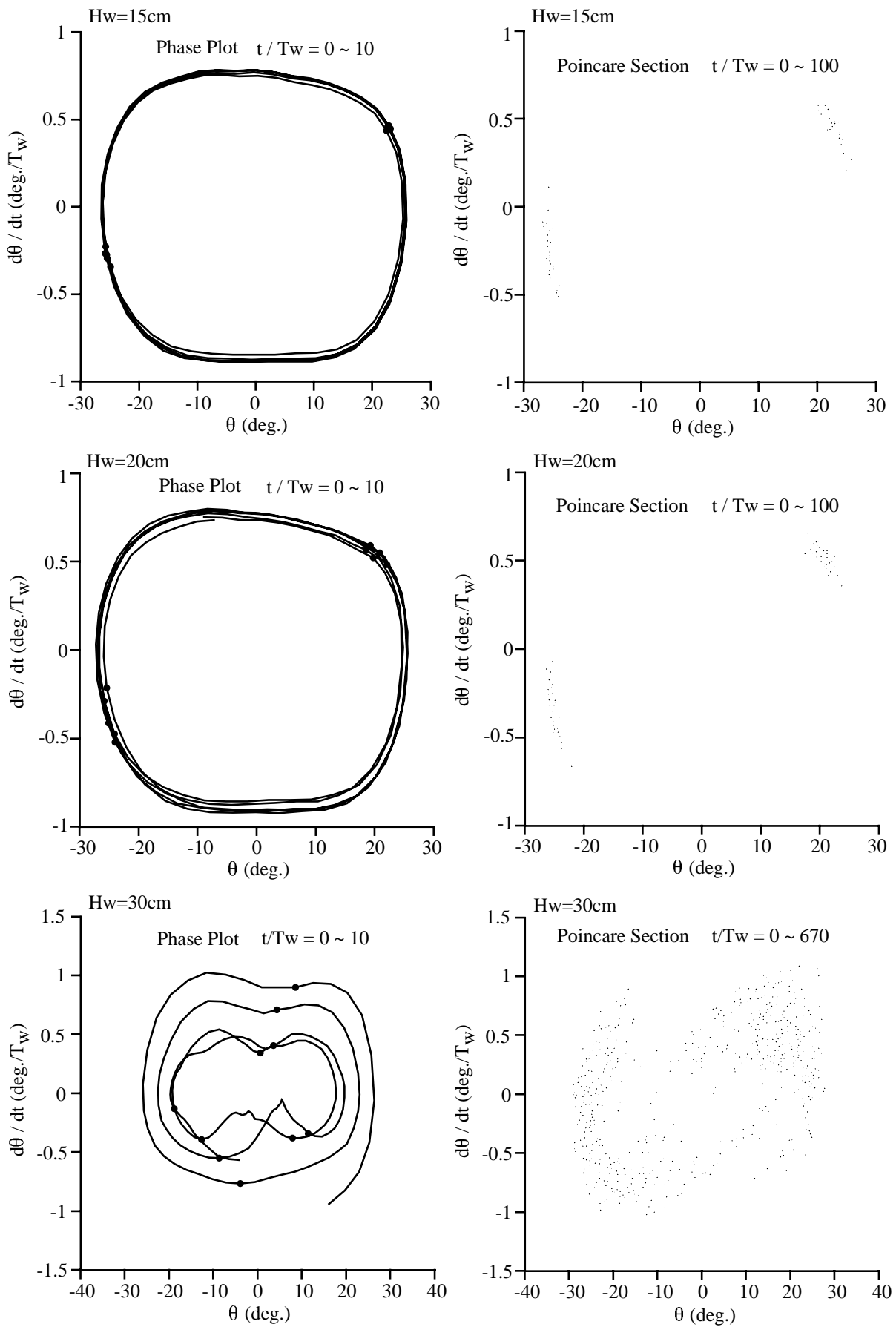


Fig.7: Phase plot and its Poncare section of the simulated roll motion

